LC lens systems to solve accommodation/convergence conflict in three-dimensional and virtual reality displays

Afsoon Jamali
Comrun Yousefzadeh
Colin McGinty
Douglas Bryant
Philip Bos

LC lens systems to solve accommodation/convergence conflict in three-dimensional and virtual reality displays

Afsoon Jamali, Comrun Yousefzadeh, Colin McGinty, Douglas Bryant, and Philip Bos*
Kent State University, Liquid Crystal Institute, Kent, Ohio, United States

Abstract. Accommodation–convergence mismatch is still an unsolved issue within the field of augmented reality, virtual reality, and three-dimensional systems in general. Solutions suggested to correct the focus cue in recent years require additional bandwidth, or compromise the image resolution. Our simple approach to overcome this issue is by using an eye-tracking system and electronic lenses. We propose an electronic hybrid lens system composed of segmented phase profile liquid crystal and Pancharatnam phase lenses. For practical application, eye tracking is necessary for measuring the toe-in of the user's pupil to calculate the object depth. This information is used to determine the required diopteric power of the hybrid system. The optical performance and imaging quality of the proposed hybrid system are evaluated. © *The Authors. Published by SPIE under a Creative Commons Attribution 3.0 Unported License. Distribution or reproduction of this work in whole or in part requires full attribution of the original publication, including its DOI.* [DOI: 10.1117/1.OE.57.10.105101]

1 Introduction

The issue of accommodation–convergence (AC) mismatch in three-dimensional (3-D) displays, particularly head-mounted displays (HMDs), causes an unnatural viewing experience and results in user discomfort. In recent years, researchers have investigated a variety of approaches to solve the AC issue. Light field displays including multiview retinal displays,[1] microlens arrays,[2] parallax barriers,[3] pinlight displays,[4] multifocal displays,[5,6] and digital holography[7] are among the main technologies that address the issue.

Light field displays project multiple perspectives of the virtual objects into different parts of pupil. To elaborate more on the requirements of light-field technology, one can consider emulation of a window by a display. The window has patches, below the resolution limit of the eye, which are replaced by pixels of a display where each pixel emits a bundle of rays, each with color and intensity corresponding to a patch in a window as shown in Fig. 1.

If several angularly distinct rays for a point in the object space are intercepted by the pupil, the eye lens will focus them to a point on the retina. The further away the point being considered, the more parallel the intercepted rays, and the lower the required eye lens power.

Takaki and Kikuta[8] showed that if a display provides enough angular resolution, the eye will focus correctly. Takaki and Kikuta[8] demonstrated a display having 0.23-deg angular resolution that was shown to provide the accommodation cue. Therefore, if a 0.2-deg angular resolution of the pixels is considered (color and intensity of each pixel can have a different value for a 0.2-deg change in angle) with an HMD that has a defined eyebox, the number of the distinct rays from each pixel can be calculated. For example, if the eyebox is 1 cm on a side, and the apparent display distance (ADD) is 0.5 m, the largest angle the pixel needs to emit will be 0.57 deg, and thus each pixel needs to emit $\left(\frac{0.57}{0.2}\right)^2$ rays or

$16 \frac{\text{rays}}{\text{pixel}}$. Therefore, the bandwidth of display must be 16 times that of a two-dimensional (2-D) display with the same pixel count for an HMD.

Love et al.[6] used a four-field sequential volumetric display (multifocal) system to provide focus cue, which requires only 4× increase in bandwidth. But the four-field sequential system is still a stretch for existing technology.

In a digital holographic display, as the projector is magnified by diverging light, the field of view increases; however, display etendue, which is the product of field of view and viewing eye box, is constant. Therefore, an increase in the field of view results in a decrease in the viewing eyebox. Small eyebox size leads to image disappearance when the eye rotates. Maimone demonstrated a digital holographic display with high image quality presenting focus cue but with about a millimeter eyebox.[7] Thus, pupil expansion is required in a digital holographic display using additional elements such as beam-steering devices.

Accommodation-invariant (AI) computational near-eye display is another approach proposed to solve AC issue.[9] AI approach is the only one-for-all solution to AC problem that has the potential to correct the refractive errors of the users; however, the image resolution is compromised.

Another solution to the AC issue is to use adaptive focus. Oculus half-dome prototype is a technology that uses adaptive focus approach. In this prototype, the display distance is mechanically changed to provide focus cue.[10] Another approach is to use a variable focus lens to change the accommodation distance of the eye.[11]

We proposed another adaptive focus approach in which the focusing power of virtual reality (VR) lens is electronically changed in combination with an eye-tracking system. It was shown that the AC issue can be solved without reduction in image resolution or the need to increase the system resolution and refresh rate.[12]

A recent study by Kramida and Varshney,[13] which performed an extensive literature review and provided assessments of benefits and limitations of each proposed

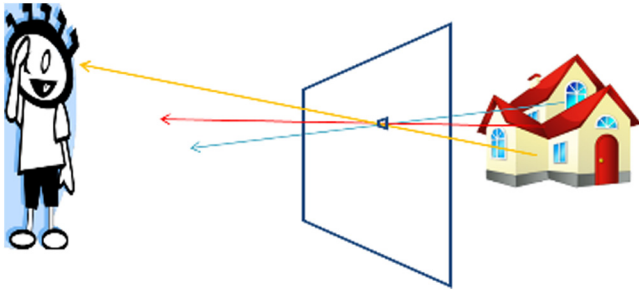*Address all correspondence to: Philip Bos, E-mail: pbos@kent.edu

Fig. 1 Illustration of emulation of a window by a display.

solution for AC problem, concluded that eye-tracked varifocal optics with LC lenses has the highest potential for solving the AC problem.

2 Virtual Reality Optics with an Adjustable Focal Length

In a conventional VR system, the lens shown in Fig. 2 has a fixed focal length, but in the system considered in this paper, the VR lens has an adjustable power. There are two conditions that are the starting points for determining the range of adjustment required. First is that the display is focused on the retina:

$$D_e + D_{VR} = \frac{1}{TDD} + \frac{1}{ED},\qquad(1)$$

where D_e and D_{VR} are the powers in diopters of the eye lens and the VR lens, TDD, ED are the display distance to the eye lens and the optical distance from the eye lens to the retina, respectively.

Second is that the eye lens will be accommodated to the ADD:

$$D_e = \frac{1}{ADD} + \frac{1}{ED}.\qquad(2)$$

Therefore, the power of VR lens is given as

$$D_{VR} = \frac{1}{TDD} - \frac{1}{ADD}.\qquad(3)$$

If we would like to electrically adjust ADD, the range of power of the VR lens is determined by the range in ADD:

$$\Delta D_{VR} = \left(\frac{1}{TDD} - \frac{1}{ADD_{max}}\right) - \left(\frac{1}{TDD} - \frac{1}{ADD_{min}}\right)$$
$$= \frac{1}{ADD_{min}} - \frac{1}{ADD_{max}}.\qquad(4)$$

Ideally, for no accommodation–convergence mismatch, ADD = AOD, where AOD is apparent object distance, so the ideal range of the power of the VR lens is given by the above equation, with AOD substituted for ADD:

$$\Delta D_{VR,min} = \frac{1}{AOD_{min}} - \frac{1}{AOD_{max}}.\qquad(5)$$

Based on Shibata et al.[14] analysis, 0.5 diopter or smaller mismatch between eye focus and convergence angle can be still considered in viewer's eyes "zone of comfort." Therefore to be within the limit of "zone of comfort," the power of VR lens may be off by 0.5 diopter thus:

$$\Delta D_{VR,min} = \left(\frac{1}{AOD_{min}} - \frac{1}{2}\right) - \left(\frac{1}{AOD_{max}} + \frac{1}{2}\right)$$
$$= \frac{1}{AOD_{min}} - \frac{1}{AOD_{max}} - 1.\qquad(6)$$

If we assume AOD_{min} is 0.5 m and AOD_{max} is infinity, then the range of power of the VR lens for perfect accommodation is 2-D [Eq. (5)], and the minimum to stay in the zone of comfort is 1-D [Eq. (6)].

To control the power of electronic lenses, eye-tracking system is used to determine the distance of the object being considered by the user. More specifically, camera
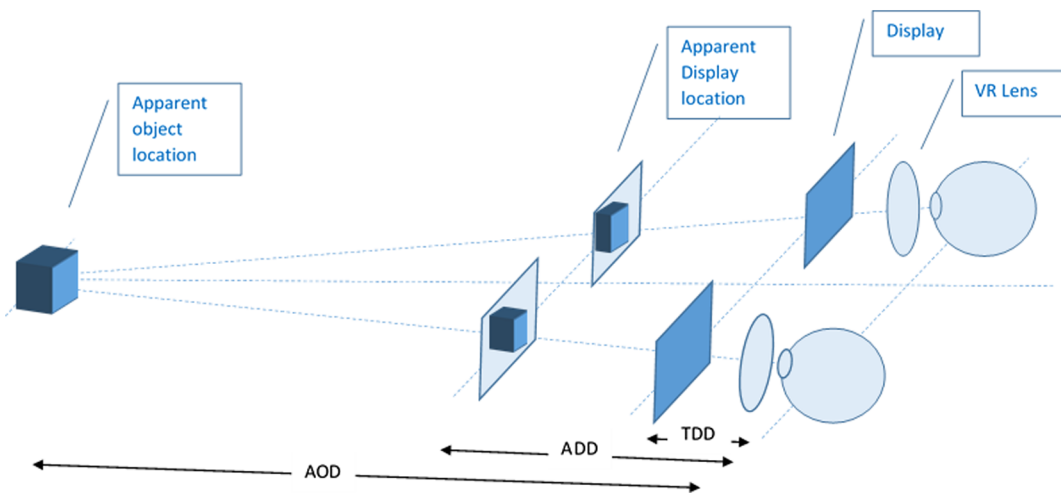

Fig. 2 Illustration of virtual reality system. TDD is the true display distance. ADD is the apparent display distance (user eyes focus at this distance by means of VR lens). AOD is the apparent object distance (left and right eye converge at this distance).

can locate the "toe-in" of pupils to determine distance from viewer to virtual object. AOD then can be obtained from x, which is the offset distance of the pupil of the eye from its location when looking an object at infinity, user's interpapillary distance (IPD), and the radius of the eye-ball (ER) as shown in [Eq. (7)]:

$$AOD = IPD \times \frac{ER}{2x}. \tag{7}$$

Therefore if an eye-tracker is used to determine the AOD of the object being considered by the user, and the range of AOD is limited to be from 0.5 m to infinity, the accommodation–convergence mismatch problem can be solved completely with a 2-D variable lens and minimally with a one-dimensional (1-D) variable lens. More details about gaze estimation using eye vergence can be found in Refs. 14 and 15. Mlot et al.[15] reported a high average accuracy of 1.2 deg using their method of tracking.

The ultimate aim in the lens design is to generate a parabolic spatial variation of the phase that causes the transmitted beams to converge to a point. Parabolic phase is acquired primarily by two main approaches. First is to control the phase gradient by the optical path difference (OPD = $\Delta n.d$, where Δn denotes the effective birefringence and d represents the thickness) and the second method for modulating the incident light is to utilize Pancharatnam phase. In the following sections, we describe LC lens design based on each of these approaches.

3 Design of the Lens System

The straightforward approach to make a tunable lens to solve the AC problem is to electrically adjust the OPD to provide a parabolic phase profile. One of the best approaches to obtain a parabolic phase profile is to use discrete concentric ring electrodes with equal area; in this case, the phase step between adjacent electrodes is a constant. An LC lens based on discrete ring electrodes has been shown to be continuously tunable and to have diffraction limited performance.[16]

A complicating issue is that for the considered application, its aperture must be large. There is a tradeoff between aperture size and response speed, and thus designing an LC lens with large aperture and reasonable response time is an uphill task.

In our recent study, we addressed this issue by introducing segments in the phase profile to increase the effective OPD without sacrificing the response time.[17] We selected the width of phase segment sufficiently large (>1 mm) thus, no observable diffraction was realized [details of design, fabrication, and characterization of the segmented phase profile (SPP) LC lens are discussed in Ref. 16]. A simple user evaluation study on the SPP LC lens was performed and is included in Appendix A. Using five resets in the phase profile, we could successfully reduce the response time by 25 times. Although the switching speed between two extreme optical powers (1.5 D and 0 D) still is about 720 ms, according to a study on human eye accommodation response,[18] the maximum accommodation rate for young people is in the range of 1.878 ± 0.0625 diopter/s, which implies our obtained response time with SPP LC lens is sufficiently fast to keep pace with eye accommodation. However, a higher power and faster response time (about 300 ms[19]) is preferred over what we have previously demonstrated.

4 Combining Segmented Phase Profile LC and Pancharatnam Phase Lenses

It is well known that the response time could be fourfold improved by stacking cells with half of thickness. By stacking four SPP LC lenses with 10-μm thickness, we could obtain continuous focus tunability between 1.5 to 0 D with 180-ms switching speed between extreme optical powers. To enhance the optical power stacking, even more cells are required. Stacking more cells raises questions regarding processing cost. What follows is the alternative solution (here we call hybrid approach) whereby we can proceed to enhance optical power without need to stack more SPP LC lenses.

4.1 Design

One of the components in the hybrid system design is Pancharatnam phase lens (PPL). PPLs are polarization sensitive lenses that can have optical power of different signs depending on the incident polarization state. Therefore by means of switchable half wave plate, one can switch between orthogonal circular polarization states of light and cause the PPL to toggle between positive and negative optical power.

The basic design of a PPL has been described elsewhere[20–24] but here we will give an idea of the structure and operation of these devices. A PPL is a thin film of a birefringent material, where the optical axis of the material is in the plane of the film while making an angle ($\beta\beta$) that is a function of the radius of the lens. The film's thickness is set by the condition $\frac{\Delta n.d}{\lambda} = \frac{1}{2}$, so that when circularly polarized light that is RHC or LHC is incident on this device the light exists as the orthogonal polarization state (either LHC or RHC, respectively). The interesting thing about this structure is that the relative phase of light exiting the aperture from any two points will have a phase difference that is given by $2\Delta\beta$, where $\Delta\beta$ is the difference in the value of β between those points. For a lens of focal length f, the phase as a function of the lens radius, r, is given as

$$\Gamma(r) = \frac{\pi r^2}{\lambda f}. \tag{8}$$

With $\Gamma(r)$ equal to $2\beta(r)$, the value of $\beta(r)$ is given as

$$\beta(r) = \frac{\pi r^2}{2\lambda f}. \tag{9}$$

This type of device has a continuous phase profile and can increase to any value, which yields devices with very high efficiency.

Perhaps the main disadvantage of PPL is the dependency of its focal length (f) to the incident wavelength (λ) as shown in Eq. (10):

$$f = \frac{\pi r^2}{2\beta(r)\lambda}, \tag{10}$$

where r and $\beta(r)$ are the lens radius and azimuthal angle of the optic axis of the half wave retarder, respectively. However, we have shown in a separate publication that with optical power less than 2-D, the chromaticy of the PPL can be considered negligible.[25]
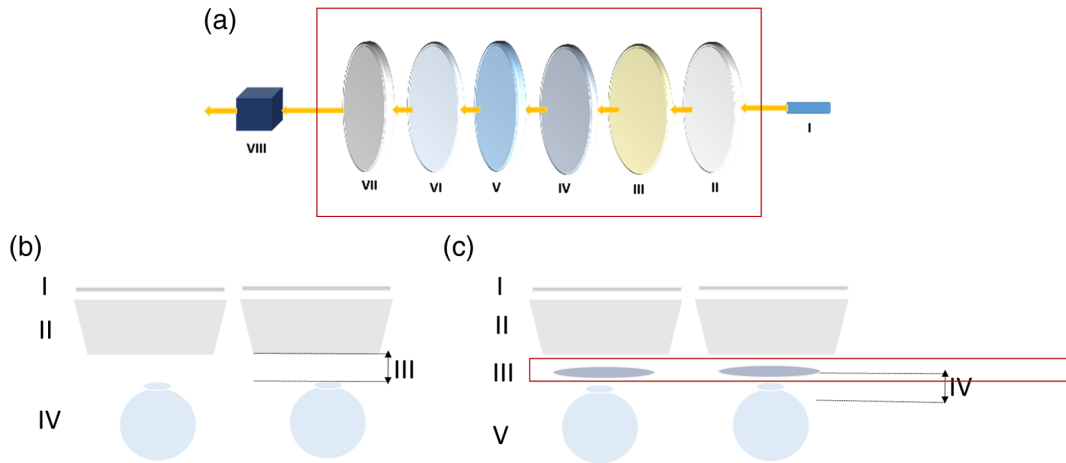
Fig. 3 (a) Designed hybrid system including I: Light source (display), II: glass lens, III: PPL, IV: switchable half wave plate, V: quarter wave plate, VI: SPP LC lens, VII: linear polarizer, VIII: imaging system (eye/CCD). (b) VR system without designed hybrid system I: VR display, II: magnifier lens mounted on optical tunnel, III: eye-relief distance, IV: eye. (c) VR system combined with the designed hybrid system, I: VR display, II: magnifier lens mounted on optical tunnel, III: variable focus hybrid system marked with red box in part A, IV: eye-relief distance, and V: eye. The entire stack of hybrid system can be made with <2-mm thickness using 0.1-mm glass substrate.

Lee et al.[26] showed that PPL can provide fast response focus for augmented and virtual reality (AR/VR) application. His proposed design has the potential to switch between two planes; however, we integrate PPL with SPP LC lenses to be able to have a continuous range of focus. Our system goal is to have a lens that is able to vary power from 0 to 2.5 D, but here, due to component availability, we construct and evaluate a system that is continuously variable from 0.375 to 2.625 D. Figure 3 shows the designed hybrid system with continuous optical power range of 2.25 D (from 0.375 to 2.625 D).

As mentioned earlier, a PPL can change power from positive to negative by changing the handedness of incident circularly polarized light. In our designed system, we first use a linear polarizer and a quarter wave plate to make the unpolarized light of real world to circularly polarized. Next, there exists an LC switchable half wave plate to change the handedness of the incident light if desired. Other optical elements in the system are the PPL with ±0.375 D, glass lens with optical power of +1.5 D, and lastly stack of two SPP LC lens with continuous tunability in the range of ±0.75 D. With this system, when the power of the PPL is −0.375 D (determined by the state of the switchable half wave plate) the system power can be varied continuously from 0.355 to 1.875 D when the SPP LC is varied from −0.75 to +0.75 D. And when the power of the PPL is +0.375 D, the system range goes from 1.125 to 2.625 as the SPP LC is varied over its range. In the other words by using the hybrid system, the optical power range is expanded coarsely by PPL (binary switching between two optical power values of +0.375 and −0.375 D) and finely by SPP LC lens (continuous tunability between +0.75 and −0.75 D). This combination enables the designed hybrid system to have continuous tunability between 0 to +2.5 D.

The design, fabrication, and application of PPL have been reported by many research groups.[17–21] The fabrication details of our PPL is included in Appendix B of this paper.

5 Characterization

5.1 Point Spread Function

We have captured the spot size of the hybrid system at the focal point for minimum and maximum optical powers. Beam size of He/Ne laser of the 543-nm wavelength was expanded by means of 10× beam expander and then through an aperture with 5-mm diameter. A canon Rebel XSi CCD sensor (camera with lens removed) was placed at the focal point to capture the spot profile. Figures 4(a) and 4(b) show the spot profile at 2.625 and 0.375 D optical powers, respectively. For each optical power state, we presented the spot profile at two exposure levels [maximum optical power (2.625 D): Figs. 4(a.1) and 4(a.2), and minimum optical power (0.375 D): Figs. 4(b.1) and 4(b.2)]. Furthermore, we showed the intensity profiles across the blue and red lines of Figs. 4(a.2) and 4(b.2) in Figs. 4(a.3), 4(a.4), 4(b.3), and 4(b.4), respectively. Black curves in these images represent the theoretical spot size. The spot size measurement shows that the deviation from theoretical spot size is insignificant and imaging performance of hybrid design is promising.

We also measured the spot profile at three intermediate power states of the hybrid system including 0.75, 1.5, and 2.25 D. In 0.75 and 1.5 D states, we added a glass lens with 1.5 and 0.75 D, respectively, to make the total optical power of system in all cases 2.25 D, which make the comparison much easier. We plotted the obtained results in Fig. 5, which shows excellent optical performance of the system in different focusing powers.

5.2 Imaging Resolution

We have evaluated the imaging resolution of our design system at its maximum and minimum optical power states using USAF 1951, which is shown in Figs. 6 and 7, respectively. The condition of each image is explained in the figure caption.
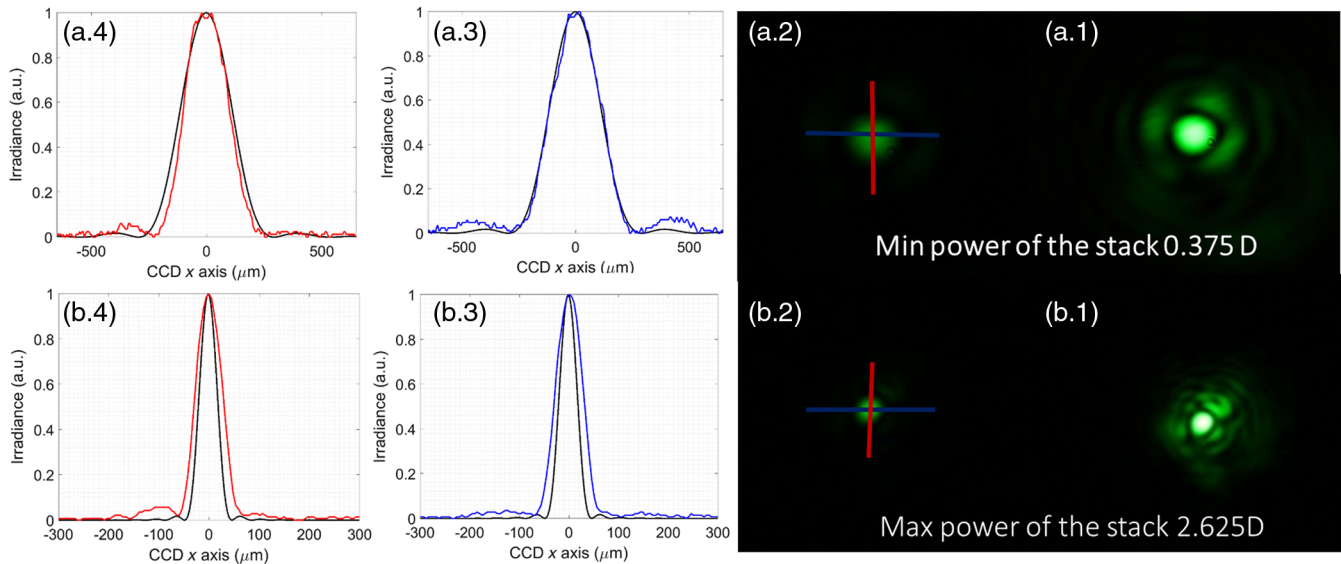
Fig. 4 (a.1) Spot size of hybrid system at 0.375 D state captured at 1/30th exposure. (a.2) Spot size of hybrid system at 0.375 D state captured at 1/3000th exposure. (a.3) Intensity profile across blue line shown in (a.2). (a.4) Intensity profile across red line shown in (a.2). (b.1). Spot size of hybrid system at 2.625 D state captured at 1/30th exposure. (b.2) Spot size of hybrid system at 2.625 D state captured at 1/3000th exposure. (b.3) Intensity profile across blue line shown in (b.2). (b.4) Intensity profile across red line shown in (b.2). The dark curves shown in graph is theoretical spot size.
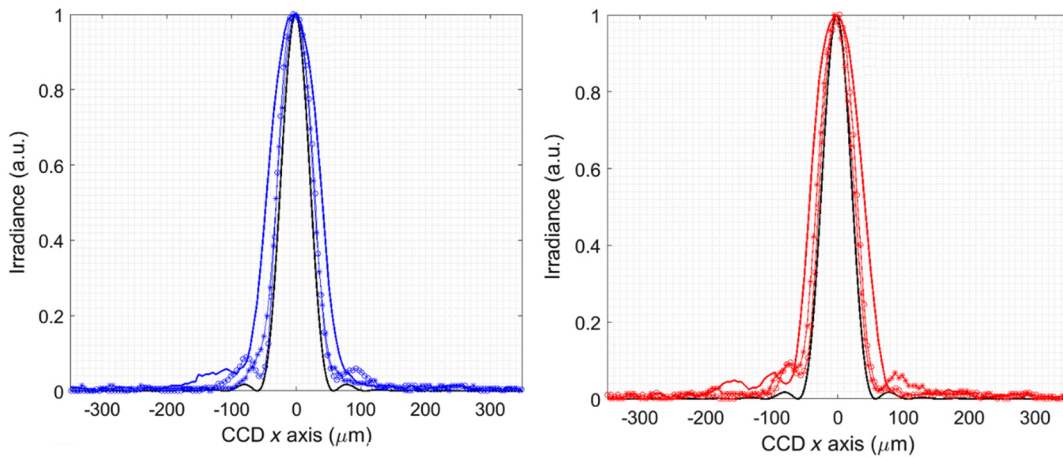

Fig. 5 Light passes through 5-mm aperture at the center of hybrid system. Three optical power states were measured with total optical power of 2.25 D, 1.5 D, and 0.75 D. For state 1.5 and 0.75 D, 0.75 and 1.5 D glass lens was added, respectively, to make the optical power 2.25 D.

6 Discussion

In considering the data shown in Fig. 5, one can realize that the solid line that indicates the PSF of the 2.25 D optical power is wider than PSF of the other two optical powers of 1.5 D (shown with lines marked with start) and 0.75 D (lines marked with circle). This is probably because the aperture size during the last experiments was <5 mm.

In assessment of data shown in Figs. 6 and 7, no chromatic aberration was observed. This was expected because of low optical power selected for PPL. Using our proposed hybrid system, we could obtain similar imaging resolution of a glass lens [Fig 6(b.2) and 6(c.2)]. The imaging resolution of the system at minimum optical power (Fig. 7) is degraded in comparison with Fig. 6, which is most probably due to the

negative phase profile of SPP LC lens that requires further voltage adjustment to be exactly parabolic. Contrast reduction also known as haze observed in the images captured by the hybrid system is due to the gap between the electrodes used in SPP LC lens. To eliminate the gap between the electrodes and thus the haze, use of "floating" electrodes that are not driven but capacitively coupled to the electrodes below are suggested previously.[15] We have demonstrated and compared the performance of SPP LC lens with and without "floating electrodes" in a separate work.[16] For the example hybrid system discussed here, the SPP LC lens used did not have "floating electrodes," which results the observed haze. This haze can be easily eliminated for practical application using the SPP LC lens with "floating" electrodes.
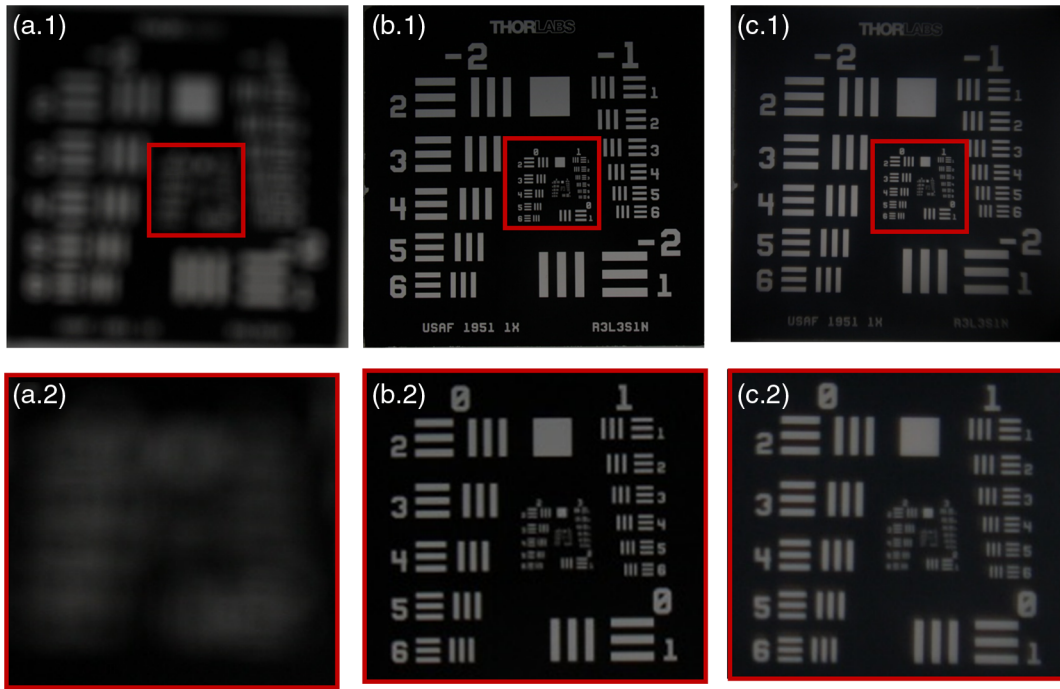
Fig. 6 The camera lens is focused at infinity. The eyechart is placed at 40.5 cm. (a.1) Image is taken with 50-mm camera lens. (b.1) Image is taken with 2.5 D glass lens plus 50-mm camera lens. (c.1) Images are taken with our designed hybrid system at 2.625 D power state plus 50-mm camera lens. The object was moved to 39.5-cm distance to find the best focus. (a.2), (b.2), and (c.2) are expanded images of the highlighted region with red square of image (a.1), (b.1), and (c.1), respectively.
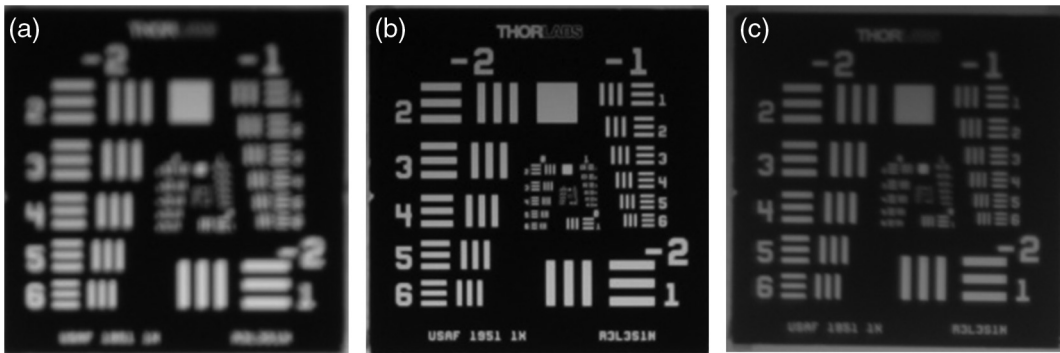

Fig. 7 The camera lens is focused at infinity. The eyechart is placed at 2 m. (a) Image is taken with 50-mm camera lens. (b) Image is taken with 0.5 D glass lens plus 50-mm camera lens. (c) Images are taken with our designed hybrid system at 0.375 D power state plus 50-mm camera lens. The object was moved to 166-cm distance to find the best focus.

7 Conclusion

In this paper, we proposed a hybrid system that consists of SPP LC and Pancharatnam phase lenses. The proposed system provides continuous tunability in the range of 0.375 to 2.625 D that can be used to solve AC issue in 3-D displays and VR systems. It should be noted that as the 3-D and VR displays are polarized, the proposed design does not reduce the transmission level of the system.

8 Appendix A: User Preference Study on Segmented Phase Profile LC Lens

Padmanaban et al.[24] performed an extensive user study demonstrating that tunable lens can correct the focus cue of near-eye display. In this section, we also present a simple user evaluation study that was performed on our designed SPP LC lens of 1.5 D optical power range.

Nvidia 120 Hz active LCD glasses-based 3-D viewing system was used in this analysis. A 3-D scene was created that consisted of three objects (wire frame cubes) placed at different distances to the user: 50 cm (object A: on screen), 80 cm (object C: 30 cm behind the screen), and 100 cm (object B: 50 cm behind the screen). The parallax corresponding to the depth of each object was rendered correctly to provide the Stereopsis cue. The Perspective and Occlusion cues were all considered when creating the scene. A stack of two SPP LC lenses (with ±0.68 D optical power) and a fixed power glass lens (with +0.75 D optical power) were added to
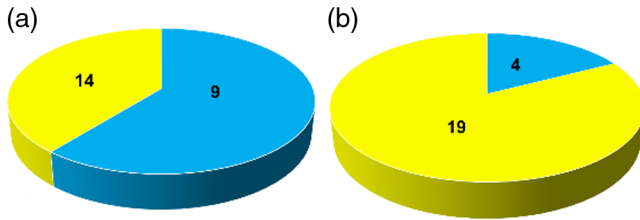
(a) (b)

Fig. 8 Preference of users in optical power states while viewing. (a) On the screen with 0.5-m distance to the user B. (b) Behind the screen with 1-m distance to the user 0.07 diopter 1.43 diopter.

the active LCD glasses. The optical power range of the stack was from 0.07 to 1.43 D.

The user was asked to sit on the chair at the distance of 50 cm to display and to wear the active glasses combined with LC/glass stack. The user was not aware of the value of optical power but was informed that there exist two conditions: (1) Diopteric power close to zero (0.07 D) and (2) higher diopteric power (1.42 D).

First, the user was reminded to only try to focus on object A for 10 s. The optical power of the SPP LC lens was adjusted to the state close to zero. Following questions were asked from user during the test. "What is the level of comfort ranging from 0 to 10 in viewing of focused object?" If the user asked us "What do you mean by the level of comfort?", we answered "It implies how clear and without any problem the 3-D scene can be seen. If your eye gets tired or you have difficulty focusing on the object, the level of comfort should be low."

In the next steps, the 1.43 D state of LC/glass stack was examined, resulting the eye to focus as if it was looking at an object at the distance of object B, rather than the distance of the display screen. Subsequently, we repeated the experiment, but this time, the user was asked to focus only on object B. The results of this study are shown in Fig. 8 This figure shows the preference of users in selecting the best power state for observing objects A and B and agrees well with the hypothesis that adding optical power to the viewers eyeware, to make the focus cue consistent with the convergence cue is beneficial to the viewing experience. These results, using LC lenses, are in line with the more controlled experiments of Padmanaban et al.[27]

9 Appendix B: Pancharatnam Phase Lens Fabrication

Mach–Zehnder interferometer is used for optical recording of spiral configuration required to fulfill the Panchartnam–Berry lens. The holographic setup consists of 457-nm laser with 3-mm beam size that is expanded to 30 mm by means of a 10× beam expander after reflecting from the mirror. The expanded beam is subsequently distributed into two arms using a beam splitter (BS) after passing through a 2-cm stop. The two diverged beams become left-handed circularly polarized by quarter wave plates (QWP) and then are merged proceeding through the beam combiner (BC). One of the two arms serves as a reference (arm 1) and the other is focused by a template lens (arm 2). The template lens in the setup is placed before the beam combiner as shown in Fig. 9. The reference path interferes with the template path to generate the spiral configuration on the glass substrate coated with alignment layer [here brilliant yellow (BY)].
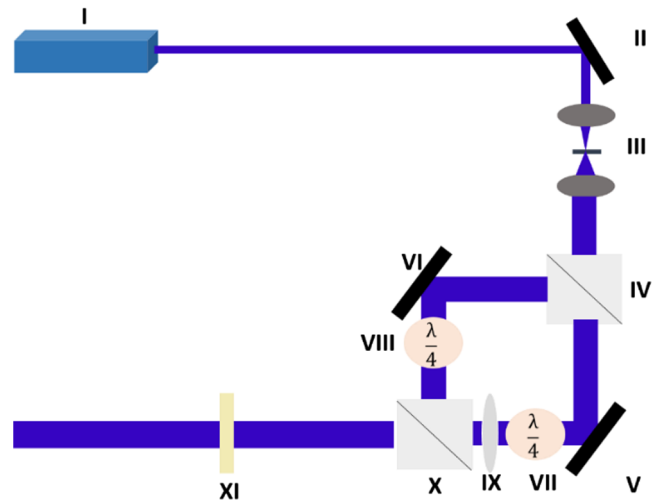

Fig. 9 Schematic depiction of the optical recording setup used for BY exposure. I: 457-nm laser, II: mirror, III: 10× beam expander, IV: beam splitter, V and VI: mirror, VII and VIII: quarter wave plate, IX: template lens with optical power of 0.25 diopter, X: beam combiner, and XI: BY coated substrate.

Prior to spinning the BY layer, the substrate is thoroughly cleaned and the surface is treated with UV/ozone for 10 min. Subsequently, 1.5% by weight BY dissolved in dimethylformamide (DMF) is spun at 3000 rpm for 30 s. Right after 15-min exposure at the discussed exposure setup, reactive mesogen (LC monomer) solution is spun at 2000 rpm for 30 s. Reactive mesogen (RM) solution contains 10% by weight RM dissolved in toluene plus photoinitiator irgacure with the amount of 5% of RM weight. After spin coating, the substrate is soft baked at 55°C for 60 s and cured with 365-nm fluorescence UV light for 7 min. The RM coating step is repeated until the thickness of the film is equal to $\frac{\lambda}{2}$.

References

1. D. W. Kim et al., "Analysis of a head-mounted display-type multifocus display system using a laser scanning method," *Opt. Eng.* **50**(3), 035006 (2011).
2. D. Lanman and D. Luebke, "Near-eye light field displays," in *Proc. of ACM SIGGRAPH*, Vol. 32, (2013).
3. D. Lanman et al., "Contentadaptive parallax barriers," in *ACM SIGGRAPH Asia*, Vol. 29 (2010).
4. A. Maimone et al., "Pinlight displays: wide field of view augmented reality eyeglasses using defocused point light sources," in *ACM SIGGRAPH*, Vol. 1 (2014).
5. K. Akeley et al., "A stereo display prototype with multiple focal distances," in *ACM SIGGRAPH '04*, Vol. 23, pp. 804–813 (2004).
6. G. D. Love et al., "High-speed switchable lens enables the development of a volumetric stereoscopic display," *Opt. Express* **17**(18), 15716–15725 (2009).
7. A. Maimone, A. Georgios, and J. S. Kollin, "Holographic near eye displays for virtual and augmented reality," *ACM Trans. Graphics* **36**(4), 1–16 (2017).
8. Y. Takaki and K. Kikuta, "3D Images with enhanced DOF produced by 128-directional display," in *13th Int. Display Workshops*, pp. 1909–1912 (2006).
9. R. Konrad et al., "Accommodation-invariant computational near-eye display," *ACM Trans. Graphics* **36**(4), 1–12 (2017).
10. Oculus Half Dome Prototype F8 2018, 2018, https://www.youtube.com/watch?v=FM7aviAhxG4&t=83s (25 September 2018).

11. K. J. Bos, "Reducing the accommodation and convergence difference in stereoscopic three-dimensional displays by using correction lenses," *Opt. Eng.* **37**(3), 1078–1080 (1998).
12. P. J. Bos et al., "A simple method to reduce accommodation fatigue in virtual reality and augmented reality displays," in *SID Digest*, pp. 354–357 (2016).
13. G. Kramida and A. Varshney, "Resolving the vergence-accommodation conflict in head mounted displays," *IEEE Trans. Visual. Comput. Graphics* **22**(7), 1912–1931 (2016).
14. T. Shibata et al., "Stereoscopic 3D display with optical correction for the reduction of the discrepancy between accommodation and convergence," *J. Soc. Inf. Disp.* **13**, 665–671 (2005).
15. E. G. Mlot et al., "3D gaze estimation using eye vergence," in *Proc. of the Int. Joint Conf. on Biomedical Engineering Systems and Technologies*, pp. 125–131 (2016).
16. L. Li et al., "Near-diffraction-limited and low-haze electro-optical tunable liquid crystal lens with floating electrodes," *Opt. Express* **21**(7), 8371–8381 (2013).
17. A. Jamali et al., "Design of a large aperture tunable refractive Fresnel liquid crystal lens," *Appl. Opt.* **57**(7), B10–B19 (2018).
18. T. E. Lockhart and W. Shi, "Effects of age on dynamic accommodation," *Ergonomics* **53**(7), 892–903 (2010).
19. T. Takeda et al., "Three-dimensional optometer III," *Appl. Opt.* **32**(22), 4155–4168 (1993).
20. G. P. Crawford et al., "Liquid-crystal diffraction gratings using polarization holography alignment techniques," *J. Appl. Phys.* **98**, 123102 (2005).
21. L. Marrucci, C. Manzo, and D. Paparo, "Pancharatnam-Berry phase optical elements for wave front shaping in the visible domain: switchable helical mode generation," *Appl. Phys. Lett.* **88**, 221102 (2006).
22. M. J. Escuti and W. M. Jones, "A polarization-independent liquid crystal spatial-light-modulator," *Proc. SPIE* **6332**, 63320M (2006).
23. L. Shi, P. F. McManamon, and P. J. Bos, "Liquid crystal optical phase plate with a variable in-plane gradient," *J. Appl. Phys.* **104**, 033109 (2008).
24. K. Gao et al., "Thin-film Pancharatnam lens with low f-number and high quality," *Opt. Express* **23**, 26086–26094 (2015).
25. C. Yousefzadeh et al., "Achromatic limit of Pancharatnam lens," *Appl. Opt.* **57**, 1151–1158 (2018).
26. Y. H. Lee et al., "Switchable lens based on cycloidal diffractive waveplate for AR and VR applications," in *SID Symp. Digest of Technical Papers*, Vol. 48, no. 1, pp. 1061–1064 (2017).
27. N. Padmanaban et al., "Gaze-contingent adaptive focus near-eye displays," in *SID Symp. Digest of Technical Papers*, Vol. 48, no. 1, pp. 23–25 (2017).

Afsoon Jamali obtained her first MS degree in chemical process engineering from the University College London in 2010 and was a research assistant at KU Leuven, before joining Kent State University. She is a PhD candidate at Liquid Crystal Institute, Kent State University. She received her second MS degree in chemical physics from Kent State University in 2015. Her current research interests include liquid-crystal devices specifically liquid-crystal lenses and beam-steering devices.

Comrun Yousefzadeh is a PhD candidate at Liquid Crystal Institute, Kent State University. He graduated with MS degree in optical physics prior to joining Kent State University. His current research interests include liquid-crystal optical devices such as liquid-crystal lenses and beam steerings.

Colin McGinty received his BS degree in physics from Loyola University Chicago, Chicago, IL. Currently, he is pursuing his PhD with the Liquid Crystal Institute, Kent State University, Kent, OH. His research focuses on novel optical liquid-crystal devices and photoalignment of liquid crystals.

Douglas Bryant is a display engineering manager at Kent State University. He obtained his MS degree in electrical engineering from the University of Southern California in 1992. His research focus is the design and fabrication of liquid-crystal devices.

Philip Bos is a professor of physics and member of the Liquid Crystal Institute at Kent State University. He obtained his PhD in physics from Kent State University in 1978, before joining Tektronix Inc., and then returning to Kent State in 1994. His research focus is optical applications of liquid crystals.